International Journal of Pharmaceutics 370 (2009) 151–159

Contents lists available at ScienceDirect

International Journal of Pharmaceutics

journal homepage: www.elsevier.com/locate/ijpharm

In vitro and *ex vivo* bioadhesivity analysis of polymeric intravaginal caplets using physicomechanics and computational structural modeling

Valence M.K. Ndesendo[a], Viness Pillay[a,*], Yahya E. Choonara[a], Riaz A. Khan[b], Leith Meyer[c], Eckhart Buchmann[d], Uwe Rosin[e]

[a] *University of the Witwatersrand, Department of Pharmacy and Pharmacology, 7 York Road, Parktown, Gauteng, 2193, South Africa*
[b] *Intergral University, Department of Industrial Chemistry, Lucknow, 226026, India*
[c] *University of the Witwatersrand, Department of Physiology, Brian Function Research Group and Central Animal Services, 7 York Road, Parktown, 2193, South Africa*
[d] *Chris Hani Baragwanath Hospital, Department of Gynaecology and Obstetrics, Bertsham, 2013, South Africa*
[e] *PharmaNatura (Pty) Ltd., Research and Development Unit, Sandton, 2012, South Africa*

ARTICLE INFO

Article history:
Received 20 October 2008
Received in revised form 1 December 2008
Accepted 3 December 2008
Available online 7 December 2008

Keywords:
Bioadhesive polymers
Intravaginal drug delivery
Textural profile analysis
Bioadhesion
Structural modeling
Excised rabbit vaginal tissue

ABSTRACT

The *in vitro* and *ex vivo* bioadhesivity of polyacrylic acid (PAA)-based intravaginal caplets was explored from a physicomechanical and chemometrical structural modeling viewpoint. An Extreme Vertices Mixture Design was constructed for analyzing the bioadhesivity of 11 matrices that were optimized. Two sets of crosslinked PAA-based matrices comprising either allyl-sucrose (AS-PAA) or allyl-penta-erythritol (APE-PAA) were explored. Powders were compressed into caplet-shaped matrices and rotational rheological analysis was performed on hydrated polymeric blends. Caplets were evaluated for bioadhesiveness using a simulated vaginal membrane (SVM) with optimized caplets further tested using freshly excised rabbit vaginal tissue. The SVM and caplets were hydrated in simulated vaginal fluid before bioadhesivity testing using a texture analyzer to determine the rupture force between the membranous substrates and hydrated caplets. Computational and molecular structural modeling deduced transient sol–gel mechanisms, chemical interactions and inter-polymeric interfacing during caplet-substrate bioadhesion. Peak adhesive force (PAF) and work of adhesion (AUC_{FD}) values for the APE-PAA caplets (1.671 ± 0.232 N; 0.0010 ± 0.0002 J) were higher than the AS-PAA caplets (1.168 ± 0.093 N; 0.00030 ± 0.0001 J) revealing superior bioadhesiveness. Similarly, rheological analysis revealed APE-PAA blends with higher viscosity and shear stress values (9×10^5 mPa/180 Pa). The optimized APE-PAA matrices adhered appreciably to rabbit vaginal tissue (PAF = 0.883 ± 0.083 N; $AUC_{FD} = (0.0003 \pm 3.5355) \times 10^{-5}$ J). Results strongly suggest that the approach may be useful for assessing the bioadhesivity of intravaginal matrices on *ex vivo* rabbit vaginal tissue with data further supported by molecular structural analysis and energy-dependant bioadhesivity modeling.

1. Introduction

The vagina serves as a potential route of bioactive delivery for local and systemic drugs as well as uterine targeting. The advantages offered by the intravaginal route are mainly due to its large surface area and rich blood supply (Desphande et al., 1992; Vermani and Garg, 2000). However, changes within the vaginal wall during the menstrual cycle and postmenopause should be considered. For postmenopausal women, a reduction of the epithelial thickness may significantly alter the original absorption rate of bioactives (Furuhjelm et al., 1980). The development of bioadhesive intravaginal drug delivery systems allows for therapeutic levels of bioactive to be maintained locally, extends the bioactive residence time within the vagina and reduces the dosing frequency and quantity of bioactive administered (Ugwoke et al., 1999; Ceschel et al., 2001). Thus, the therapeutic efficacy of locally acting bioactives may be improved due to the increased availability at the vaginal epithelium through bioadhesion (Mandal, 2000; Genc et al., 2000; Elson et al., 2000; Bilensoy et al., 2006).

Polymers represent a class of ubiquitous materials used for intravaginal drug delivery (Lehr, 2000; Lee et al., 2000; Valenta et al., 2001, 2002; Kast et al., 2002; Tang et al., 2005; Bonferoni et al., 2006; Al-Tahami and Singh, 2007). Examples of these include bioadhesive glyminox and cecropin gels for contraception and prevention of sexually transmitted infections, terbutaline gel for dysmenorrhea and endometriosis, tenofovir gel and an antibody III-174 vaginal implant for the prevention and treatment of herpes simplex virus-2 infection (Nelson, 2008). Bioadhesive materials comprise a range of synthetic, semi-synthetic or natural poly-

* Corresponding author. Tel.: +27 11 717 2274; fax: +27 11 642 4355.
E-mail address: viness.pillay@wits.ac.za (V. Pillay).

0378-5173/$ – see front matter © 2008 Elsevier B.V. All rights reserved.
doi:10.1016/j.ijpharm.2008.12.001

mers. Currently, the majority of bioadhesive polymers include polyacrylic acid and cellulose derivatives, poly(vinylpyrrolidone) (PVP), poly(vinylalcohol) (PVA), chitosan and various gum-based polymers such as xanthan gum. Multifunctional polymers exhibiting bioadhesive and/or gelling properties such as the thiolated polyacrylates and poloxamers represent a useful framework for the design of intravaginal drug delivery systems (Bogentoft and Carlsson, 1996; Robinson and Bologna, 2002). Drug delivery systems comprising such polymers include vaginal tablets, rings and gels (Wong et al., 1999).

Bioadhesivity is essentially defined as the interfacial force between the polymeric drug delivery system and the mucus layer coating an epithelium (Peppas and Buri, 1985). Bioadhesion may occur in three distinct phases namely wetting, interpenetration and subsequent mechanical interlocking between mucin and the polymer (Longer and Robinson, 1986; Jast et al., 2003). Bioadhesion is thus thought to be a result of the presence of hydrogen bonding groups, strong anionic/cationic charges, high molecular mass, chain flexibility and surface energy interactions which favor spreading onto the vaginal tissue. Basic theories such as electronic, adsorption, wetting and diffusion phenomena have been described and associated with the mechanisms by which bioadhesion occurs (Helfand and Tagami, 1972; Kaelble, 1977; Deryaguin et al., 1997). Each of the steps involved in bioadhesion may be facilitated by the polymeric composition of the drug delivery system and the mode of application (Hussain, 2000). However, a comprehensive chemometric molecular understanding of the mechanisms by which certain macromolecules adhere to the vaginal mucosal tissue surface is not yet available (Mikos and Peppas, 1990; Valenta, 2005). Several techniques for the *in vitro* assessment of bioadhesion have been explored and include tensile testing (Park and Robinson, 1987), shear stress testing (Smart et al., 1984), adhesion mass methods (Smart and Kellaway, 1982), fluorescent probe methods (Park and Robinson, 1984), flow channel techniques (Mikos and Peppas, 1986) and colloidal gold staining methods (Park, 1989). However, these techniques lack enough sensitivity. For instance, during tensile testing the distance travelled by the upper moving platen prior to detaching from the lower stationary platen as well as the time elapsed is not adequately considered. Furthermore previous techniques employed for bioadhesivity testing could only provide one dimensional data analysis of bioadhesivity in terms of the force (Santos et al., 1999; Repka and McGinity, 2001).

Therefore this study investigated the use of a comprehensive multi-dimensional approach including chemometrical molecular modeling and pertinent mathematical descriptors to assess the polymeric bioadhesivity to vaginal tissue. The area under the force-distance curve (AUC_{FD}) under a global locale was computed for all data points iterated during bioadhesion testing of optimized polyacrylic acid (PAA)-based intravaginal matrices generated through an Extreme Vertices Mixture Experimental Design template. Bioadhesivity testing was conducted on both a simulated vaginal membrane and freshly excised rabbit vaginal tissue. Various polymers were selected based on the potential for modulating drug release, ensuring matrix integrity, desirable erodability, homeostatic control of the vaginal environment and bioadhesivity potential. The polymers included polyamide 6,10, (PA 6,10), polyethylene oxide (PEO), poly lactic co-glycolic acid (PLGA), carrageenan (CG) and polyacrylic acid (PAA). Studies have shown that PAA is a highly bioadhesive polymer (Semalty and Semalty, 2008). Thus, for comparison purposes this study explored two combinatory matrices comprising PAA of the allyl sucrose-crosslinked PAA (AS-PAA matrix) and allyl penta erythritol-crosslinked PAA (APE-PAA matrix) type as a paradigm for assessing the bioadhesivity of the selected polymer blends termed as the "AS-PAA" and "APE-PAA" Caplets" throughout this work.

2. Materials and methods

2.1. Materials

Polyamide 6,10 (PA 6,10) was synthesized using hexamethylenediamine (M_w = 116.2 g/mol), and sebacoyl chloride (M_w = 239.1 g/mol) purchased from Sigma–Aldrich Chemie GmbH (Steinheim, Germany). Polyacrylic acid (Carbopol® 934 and 974) (Noveon Inc., Cleveland, OH, USA), carrageenan (Type 1κ and α, Sigma–Aldrich Chemie, Steinheim, Germany), polyethylene oxide (Union Carbide Corp., Danbury, CT, USA) and poly(lactide-co-glycolide) (Resomer® RG504, Boehringer Ingelheim PharmKG, Ingelheim, Germany) were the polymers investigated. Albumin Bovine Serum was purchased from Sigma–Aldrich Chemie (Steinheim, Germany). The simulated vaginal membranes were dialysis flat sheet membranes of M_w = 12,000–14,000 g/mol purchased from Spectrum Laboratories Inc. (Rancho Dominguez, CA, USA). Rabbit vaginal tissue was excised from euthanized New Zealand White (NZW) Rabbits obtained from the University of the Witwatersrand Central Animal Services Unit. All other reagents were of analytical grade and used as purchased.

2.2. Synthesis of a modified polyamide 6,10 variant

A polyamide 6,10 variant was synthesized using a modified interfacial polymerization approach (Kolawole et al., 2007) employing a select combination of hexamethylenediamine (HMD), sebacoyl chloride (SC), hexane (HXN), cyclohexane (c-HXN), sodium hydroxide (NaOH) and deionized water (DW). Briefly, two monomeric solutions were prepared comprising specific quantities of HMD and NaOH dissolved in DW and another comprising SC dissolved in a mixture of HXN and c-HXN (Table 1). The organic SC solution was gradually added to the aqueous HMD blend to form a polymeric film at the interface which was collected as a mass by gradual rotation of a glass rod immersed at the interface prior to washing in HXN to remove any un-reacted SC and thereafter DW (3 × 300 mL) to remove any un-reacted NaOH. The polymeric mass was then dried to constant mass at 40 °C over 48 h prior to further blending and caplet compression.

2.3. Preparation of the allyl sucrose and allyl penta erythritol-crosslinked PAA caplets

An Extreme Vertices Mixture Design experimental formulation template was generated employing Minitab®, V15 (Minitab® Inc., PA, USA) statistical software to produce various caplet formulations comprising 11 polymer combinations (Table 2). Each formulation had an equivalent mass of 600 mg. Formulation response optimization was performed using an inherent D-optimal technique by combining mixture components and processing factors to converge to pre-optimal settings prior to achieving a global optimized

Table 1
Reactant mass and volume constituents employed for PA 6,10 variant synthesis.

HMD[a] (g)	1.75
SC[b] (g)	0.63
DW[c] (mL)	10.00
HEX[d] (mL)	40.00
C–HXN[e] (mL)	40.00
NaOH[f] (g)	0.10

[a] Hexamethylenediamine.
[b] Sebacoyl chloride.
[c] Deionized water.
[d] Hexane.
[e] Cyclohexane.
[f] Sodium hydroxide.

Table 2
Extreme Vertices Mixture Design formulation template for caplet preparation.

Formulation number	PA 6,10 (mg)	PLGA (mg)	PEO (mg)	AS-PAA[a] (mg)	APE-PAA[b] (mg)	CG (mg)
1	150	50	100	200	200	100
2	100	50	150	200	200	100
3	100	50	100	250	250	100
4	130	55	105	205	205	105
5	105	80	105	205	205	105
6	100	100	100	200	200	100
7	105	55	105	205	205	130
8	105	55	105	230	230	105
9	110	60	110	210	210	110
10	100	50	100	200	200	150
11	105	55	130	205	205	105

[a] AS-PAA: allyl sucrose-crosslinked PAA.
[b] APE-PAA: allyl penta erythritol-crosslinked PAA.

solution with the desirable polymeric proportions for the AS-PAA and APE-PAA caplets that were subsequently prepared and further tested.

The various polymers were weighed in triplicate and subsequently blended with magnesium stearate (0.5%w/w) using a cube blender (Erweka Apparatebau, Heusenstamm, Germany). The blends were then granulated with 96.5% ethanol and dried at room temperature (21 °C) over 24 h prior to compression into caplets using a Manesty D3B 16 Station Tableting Machine (Manesty D3B L249LQ, Liverpool, England) equipped with D3B oblong tooling of 9 mm × 22 mm in dimension at a compression pressure of 25 tons.

2.4. In-process validation tests of caplets

Diametric hardness, friability and mass uniformity analyses were conducted on the caplet formulations to ensure adequate manufacturing reproducibility. A sample of 10 caplets from each formulation batch was tested for diametric hardness using a Hardness Tester (Pharma Test, Hainburg, Germany), and for friability using a Friabilator (Heusenstamm, Germany), set at 1% as the upper limit of friability.

2.5. Assessment of caplet bioadhesivity

Bioadhesivity testing was performed on all experimental formulation batches and both sets of optimized caplets (i.e. the AS-PAA and APE-PAA caplet formulations) using a highly sensitive Texture Analyzer (TA.XTplus, Stable Microsystems, UK). This approach was employed to principally measure the bioadhesiveness using a cylindrical probe that was robotically guided to make contact and induce a test force onto the non-deformed substrate surface comprising either a simulated vaginal membrane or freshly excised rabbit vaginal tissue and thereafter disengage in order to simultaneously measure the force of probe detachment. The maximum force required to detach the simulated vaginal membrane attached to the cylindrical probe from the secured caplet matrix on the platen was obtained from the peak adhesive force (PAF) and also computed from the AUC_{FD} representing the work of adhesion. In each case, the simulated vaginal membrane and the caplets were hydrated for 30 min in simulated vaginal fluid (pH 4.5; 37 °C) (Table 3) prior to testing ($N = 3$). For further method and formulation validation bioadhesivity testing was also conducted using freshly excised vaginal tissue obtained from a New Zealand White rabbit model on the optimized APE-PAA caplets which displayed superior bioadhesion to the AS-PAA caplets. The textural analysis parameter settings employed were a pre-test speed and test speed = 2.0 mm s^{-1}, a post-test speed = 10 mm s^{-1}, a trigger force = 0.49033 N and a contact time of 5 s.

2.5.1. Removal of vaginal tissue from the rabbit model for bioadhesivity testing

A New Zealand White adult female rabbit (3.5 kg) was euthanized with intravenous sodium pentobarbitone (200 mg/kg) via the marginal ear vein. The pelvic canal of the rabbit was opened through the symphysis pubis to expose the intra-abdominal vaginal tract (vestibulum). The external vaginal tract was carefully dissected from the surrounding tissues before removing the vaginal tissue. An incision was made through the vaginal canal to expose the epithelium. The vaginal tissue was stored in an airtight specimen jar and immediately subjected to bioadhesivity testing.

2.5.2. Ex vivo bioadhesivity analysis of the optimized APE-PAA caplets

The freshly excised vaginal tissue was secured onto a cylindrical textural probe of a Texture Analyzer (TA.XT*plus*, Stable Microsystems, UK). An optimized APE-PAA caplet was fixed onto the textural platen after exposure to simulated vaginal fluid (pH 4.5; 37 °C) for 30 min. Bioadhesive testing was then conducted immediately by measuring the maximum force (N) required to detach the vaginal tissue from the hydrated APE-PAA caplet matrix. Data was represented as the PAF and the work of adhesion (AUC_{FD}) (Fig. 1). The work of adhesion per unit area ($wA_{\alpha\beta\delta}$), was characterized by the work executed on the matrices when the two contact phases i.e. the vaginal tissue (α) and the caplet matrix (β), formed an interface of unit area which were subsequently separated reversibly to form unit areas of each of the $\alpha\delta$- and $\beta\delta$-interfaces. This relationship is mathematically described Eq. (1).

$$wA_{\alpha\beta\delta} = \gamma\alpha\delta + \gamma\beta\delta - \gamma\alpha\beta \quad (1)$$

where $\gamma\,\alpha\beta$, $\gamma\,\alpha\delta$ and $\gamma\,\beta\delta$ are the surface tensions between the two bulk phases comprising the vaginal tissue and the APE-PAA caplet matrices, $\alpha - \beta$; $\alpha - \delta$ and $\beta - \delta$ respectively.

Table 3
Composition of simulated vaginal fluid employed.

Component	Quantity (g/L)
NaCl	3.51
KOH	1.40
$Ca(OH)_2$	0.222
Bovine serum albumin	0.018
Lactic acid	2.00
Acetic acid	1.00
Glycerol	0.16
Urea	0.4
Glucose	5.0

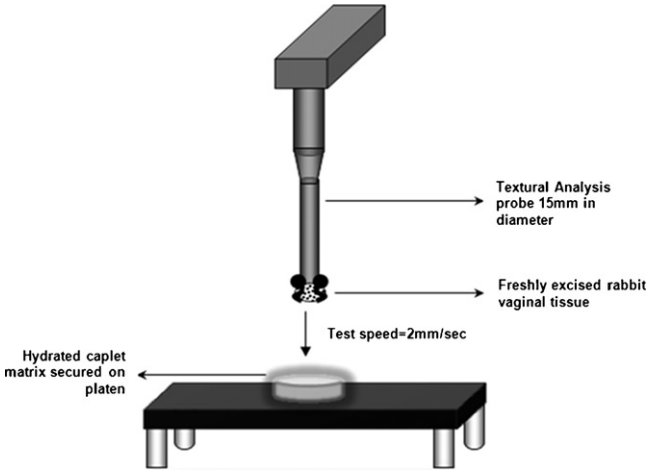

Fig. 1. Schematic diagram of the textural analysis method employed to generate force–distance profiles for assessing the caplet bioadhesivity to freshly excised rabbit vaginal tissue.

2.6. Rheological analysis of gelated AS-PAA and APE-PAA caplet matrices

The ability of PAA to partially hydrate within the caplet matrix ultimately results in wetting and volumetric distension of the system which facilitates the intimate contact and interaction with the simulated vaginal membrane and freshly excised rabbit vaginal tissue. Rotational rheological analysis was therefore performed to generate flow curves for analyzing relationships between the viscosity and shear stress as a function of shear rate using a Modular Advanced Rheometer system (ThermoHaake MARS Rheometer, Thermo Fischer Scientific, Karlsuhe, Germany) equipped with a T-type spindle sensor (C35/1° Ti) set at a sample gap of 1 mm and a Thermocontroller (UTC-MARS II). The AS-PAA and APE-PAA polymers were dissolved in simulated vaginal fluid at a concentration of 2%w/v, vortexed for 2 min, and then assessed for their rheological behaviour at $25 \pm 1.0\,^{\circ}C$ with a test time of 200 s and a controlled rate starting at $5.00\,s^{-1}$ decreasing to $0.001\,s^{-1}$ and a shear rate ranging from $0\,s^{-1}$ to $500\,s^{-1}$.

2.7. Mechanistic deduction of caplet bioadhesion employing chemometric molecular modeling and associated interactive energy paradigms

Computational and molecular structural modeling was performed to deduce the transient mechanisms of bioadhesivity, chemical interactions and inter-polymeric interfacing during caplet adhesion to the freshly excised rabbit vaginal tissue as the adhesive substrate. This approach led to predictive findings solely based on the chemical interactions underlying the bioadhesion of the caplet to the vaginal tissue substrate. Semi-empirical quantum mechanics was used to generate molecular interactions and computational energy paradigms of the caplet components based on inherent interfacial phenomena underlying the mechanisms of bioadhesion provided by the inter-polymeric blended caplet. Models and graphics supported on the step-wise molecular caplet-tissue interaction, polymeric interconversion and bioadhesion as envisioned by the molecular behaviour and stability of the gelated caplet network were generated on ACD/I-Lab, V5.11 (Add-on) software (Advanced Chemistry Development Inc., Toronto, Canada, 2000). The energy distribution curves assumed a componential progression of bioadhesion stability, a spatially uniform distribution of polymers within the caplet, and an irreversible gelation process (Yu and Quinn, 1998; Schroeder et al., 1998; Picout et al., 2000a,b; Kalugin et al., 2001; Gilsenan et al., 2003a,b,c).

Cellular adhesion may also play a critical role toward the mechanisms of achieving superior bioadhesion. While a number of computational models and experimental studies have addressed the issue of cell adhesion to surfaces, no model or theory has adequately addressed cell adhesion at the molecular level employing freshly excised rabbit vaginal tissue as the bioadhesive substrate. Therefore a thermodynamic model that addresses receptor-mediated cell adhesion at the molecular level was explored. By incorporating the entropic, conformational, solvation, and long- and short-range interactive components of receptors and the extracellular matrix molecules, adhesive free energy as a function of a number of key variables such as surface coverage, interaction distance, molecule size, and solvent conditions were predicted. This allows the computation of the free energy of adhesion in a multi-component system in order to simultaneously elucidate adhesion receptors and ligands of different sizes, chemical identities, and conformational properties. This approach not only provides a fundamental understanding of adhesion at the molecular level but may also aid in identifying possible strategies for designing novel biomaterials to improve bioadhesion of the caplet to the rabbit vaginal tissue substrate.

3. Results and discussion

3.1. PA 6,10 synthesis, caplet preparation and in-process validation tests

A total yield of 90% PA 6,10 was obtained after the interfacial polymerization reaction. The synthesized PA 6,10 presented as a robust white to off-white crystalline compact with sphere-like solids and irregular edges. The unrefined PA 6,10 powder was subsequently sieved through an aperture size of 1 mm in comparison with the other polymeric components of the caplet matrix to obtain a pseudo-polymer size ranging from 0.8 mm to 1.2 mm that facilitated desirable powder compression for caplet formation. The resultant caplets were sufficiently strong and compact with average hardness values of 286 ± 0.01 N ($N = 10$). The caplets presented ideal uniformity in mass (600 ± 0.48 mg; $N = 10$) and friability values with an average of 0.29% ($N = 10$) which was within the set limit.

3.2. Assessment of caplet bioadhesivity

Work of adhesion values for the APE-PAA caplets was significantly higher than those of AS-PAA caplets. The difference in work of adhesion was 94.1% (Fig. 2). This clearly indicated that the APE-PAA caplets had superior bioadhesivity than the AS-PAA caplets. The difference in bioadhesivity may be due to the variation in the crosslinking approach employed for the commercial synthesis of AS-PAA and APE-PAA. AS-PAA is crosslinked with allyl sucrose while APE-PAA is crosslinked with allyl penta erythritol which has superior crosslinking ability and therefore produces an intense gelated network capable of facilitating superior bioadhesion.

3.3. Response optimization and textural analysis of the optimized AS-PAA and APE-PAA caplets

Response optimization of the AS-PAA and APE-PAA caplets using Minitab® V15 (Minitab® Inc., PA, USA) software revealed the optimum level for each polymer (PA 6,10, PEO, PLGA, CG and PAA) within the caplets in order to provide the most desirable relative bioadhesivity (Fig. 3). The work of adhesion values for the optimized caplets displayed significantly higher bioadhesivity values compared to the pre-optimized APE-PAA caplets and AS-PAA caplets (Table 4). The difference in bioadhesivity between the AS-PAA and

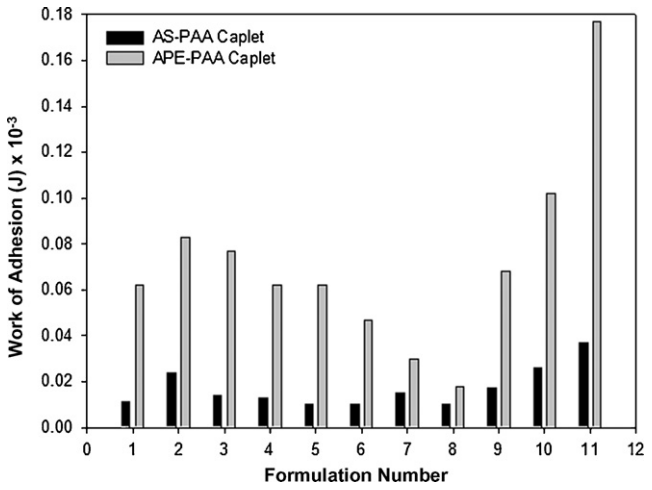

Fig. 2. A comparison of work of adhesion (AUC_{FD}) (J) between the AS-PAA and APE-PAA caplets.

APE-PAA caplets was 46.7% (Fig. 4). The desirability (D) values were 0.98 and 0.92 respectively indicating the sufficient convergence of data toward an optimized global solution.

3.4. *Ex vivo* bioadhesivity analysis of the optimized APE-PAA caplets on freshly excised vaginal tissue

The PAF value obtained was 0.883 ± 0.08273 N while the work of adhesion (AUC_{FD}) was $(0.0003 \pm 3.53553) \times 10^{-5}$ J. The results portrayed a close correlation between the PAF and the work of adhesion (Table 4). The optimized caplet matrices with desirability (D) values close to 1 disclosed the close correlation between the fitted and the experimental results (Table 4). Fig. 5 depicts a typical force–distance textural profile obtained for computing the PAF and work of adhesion values on the freshly excised vaginal tissue.

Table 4
Correlative bioadhesivity results for the pre-optimized and optimized caplets.

Textural parameters	Fitted	Experimental
In vitro analysis of optimized AS-PAA and APE-PAA caplets		
Force of adhesion (N)		
AS-PAA caplet	1.30000	1.16810 ± 0.09327
APE-PAA caplet	2.00000	1.67160 ± 0.23221
Work of adhesion (J)		
AS-PAA caplet	0.00050	0.00032 ± 0.00013
APE-PAA caplet	0.00090	0.00060 ± 0.00021
Ex vivo analysis of the optimized APE-PAA caplet		
Force of adhesion (N)	1.00000	0.88300 ± 0.08273
Work of adhesion (J)	0.00035	0.00030 ± 3.53553

3.5. *Rheological analysis of the gelated AS-PAA and APE-PAA caplet matrices*

AS-PAA and APE-PAA are polymers that are able to produce mucilages with short rheological flow properties that can be associated with the high degree of crosslinking in both polymers. In terms of rheological properties, APE-PAA was found to be highly viscous (900×10^{-3} m Pa s) in comparison to AS-PAA (80×10^{-3} m Pa s) with a subsequent higher shear stress (180 Pa vs. 58 Pa) (Fig. 6). Justifiably, this rheological observation may explain the superior bioadhesivity of the APE-PAA caplets over the AS-PAA caplets. In both cases the viscosity decreased as the shear rate increased (Fig. 6).

The bioadhesivity behavior of the caplet matrices to the freshly excised rabbit vaginal tissue is a typical reflection of the fact that the polymer combination employed for matrix formation typically

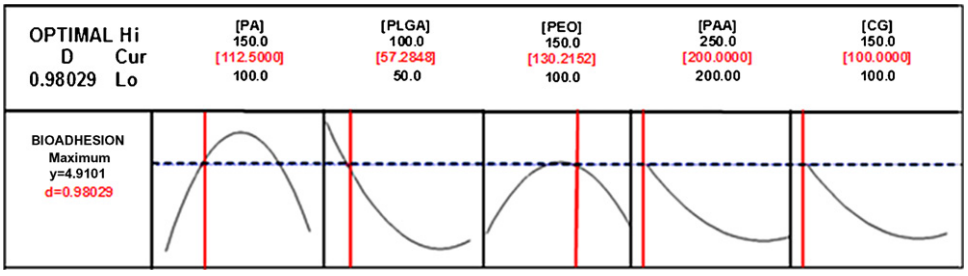

Fig. 3. A typical response optimization plot for the AS-PAA and APE-PAA caplets.

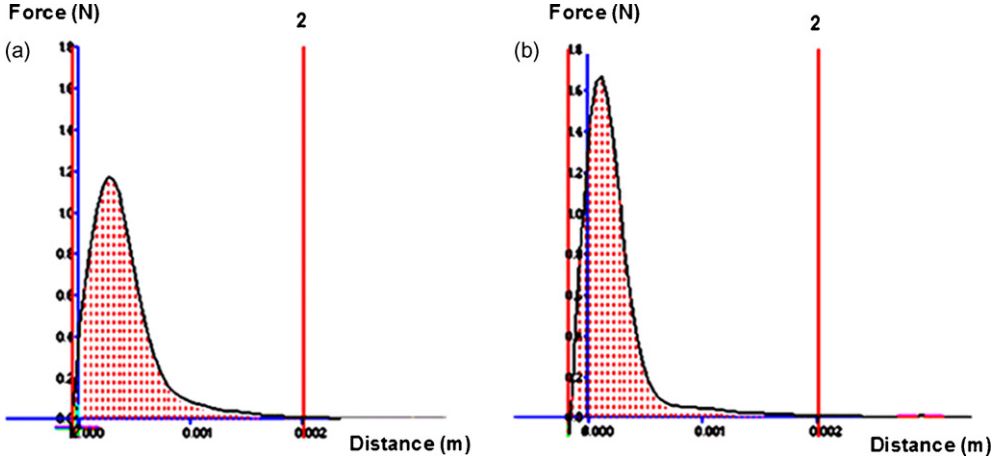

Fig. 4. Typical textural profiles elucidating the PAF (N) and work of adhesion (AUC_{FD}) (J) for the optimized (a) AS-PAA and (b) APE-PAA caplets.

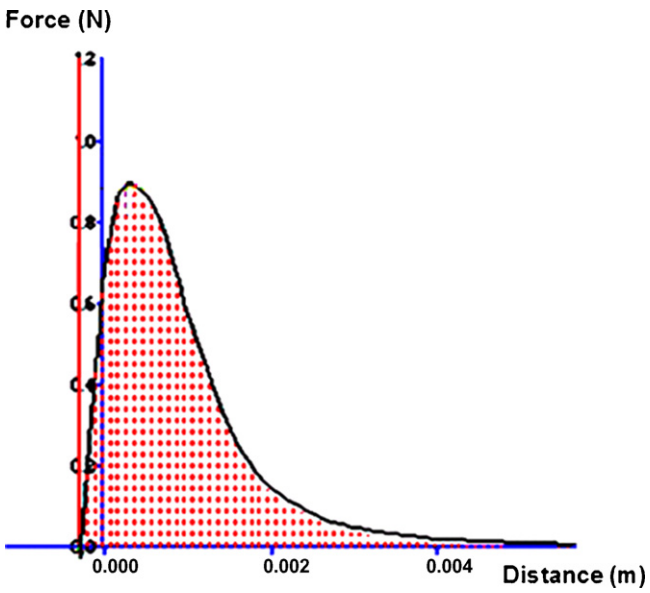

Fig. 5. Typical textural profile elucidating the force (N) and work of adhesion (AUC_{FD}) (J) for the optimized APE-PAA caplets on freshly excised vaginal tissue.

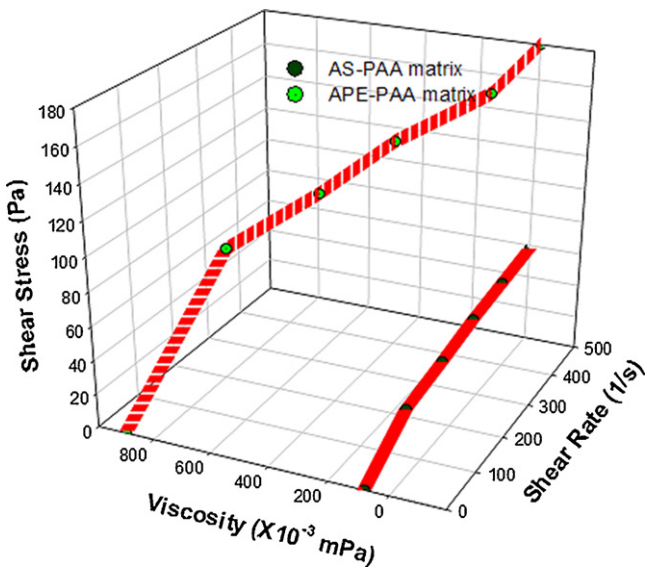

Fig. 6. Rheological behaviour of 2%w/v AS-PAA and APE-PAA solutions at a shear rate between 0 s^{-1} and 500 s^{-1}.

possesses rather different structural deformation mechanisms due to their backbone nature, molecular mass, polymeric concentration, chain flexibility, spacial conformation, pH of volumetric distention at the polymer–substrate interface, the associated forces, the initial contact time and the extent of mucin turn-over. This may be as result of their variation in moduli and rheological deformation energies. Hence deformation or flow at the polymer–vaginal tissue substrate interface occurred within the polymeric matrix with subsequent failure at the interface to induce and control the degree of bioadhesion between the caplet matrices and the freshly excised vaginal tissue.

3.6. Chemometric and molecular modeling of the mechanisms of caplet bioadhesion and the associated interactive energy paradigms

Results obtained from chemometric and computational analysis of the associated energy paradigms have revealed that the caplet bioadhesivity to the freshly excised rabbit vaginal tissue substrate may be explained in terms of the Differential Adhesion Hypothesis (DAH) theory of cell adhesion (Steinberg, 1996). The rabbit vaginal tissue substrate acted as a viscoelastic flexible semi-solid with a tissue surface tension corresponding to a mutual classification behavior occupying an internal position relative to the gelated caplet with a lower surface tension during interaction. Quantitative energy variations in homo- and heterotypic bioadhesion were sufficient to account for the phenomenon without the need to postulate cell-type specific bioadhesion. The caplet bioadhesion occurred in a stepwise mechanism involving weak inter-atomic and inter-molecular physical forces that interplay at the outset (Fig. 7).

During initial contact of the caplet with the freshly excised rabbit vaginal tissue substrate mechanical bioadhesion occurred with all surface voids between the caplet and tissue substrate filled and therefore resulted in surface interlocking. As the caplet hydrated a more unyielding chemically adhesive interaction progressed between the hydrated inter-polymeric blend of the caplet to form a bioadhesive compound at the interface either through ionic or covalent bonding prior to caplet dispersion. In the dispersive phase of bioadhesion the gelated caplet and vaginal tissue substrate were bound by van der Waals forces as a result of polymeric ionic species generated due to disentanglement and volumetric distention of the constituent polymers. In the simplest case, molecules during this phase of bioadhesion were polar with respect to the average charge density and may be due to Keesom forces or a tran-

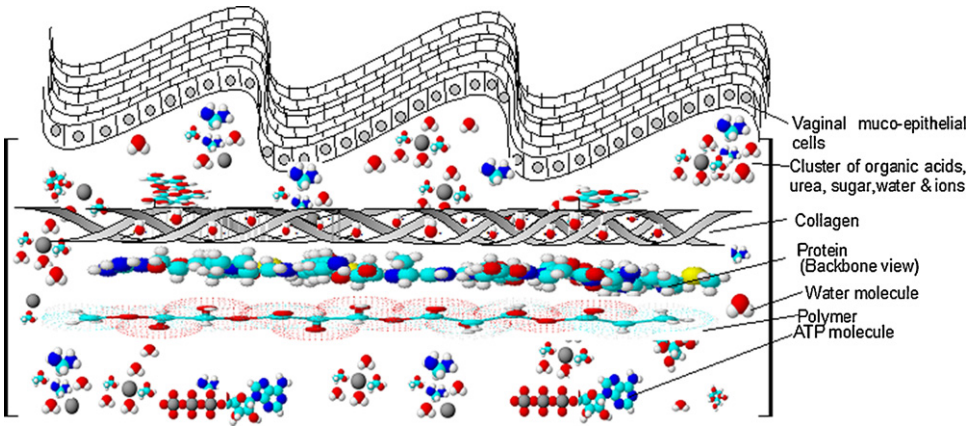

Fig. 7. A chemometric structural model depicting caplet bioadhesion to freshly excised rabbit vaginal tissue with muco-epithelial cell secretions and surface bio-molecule interactions.

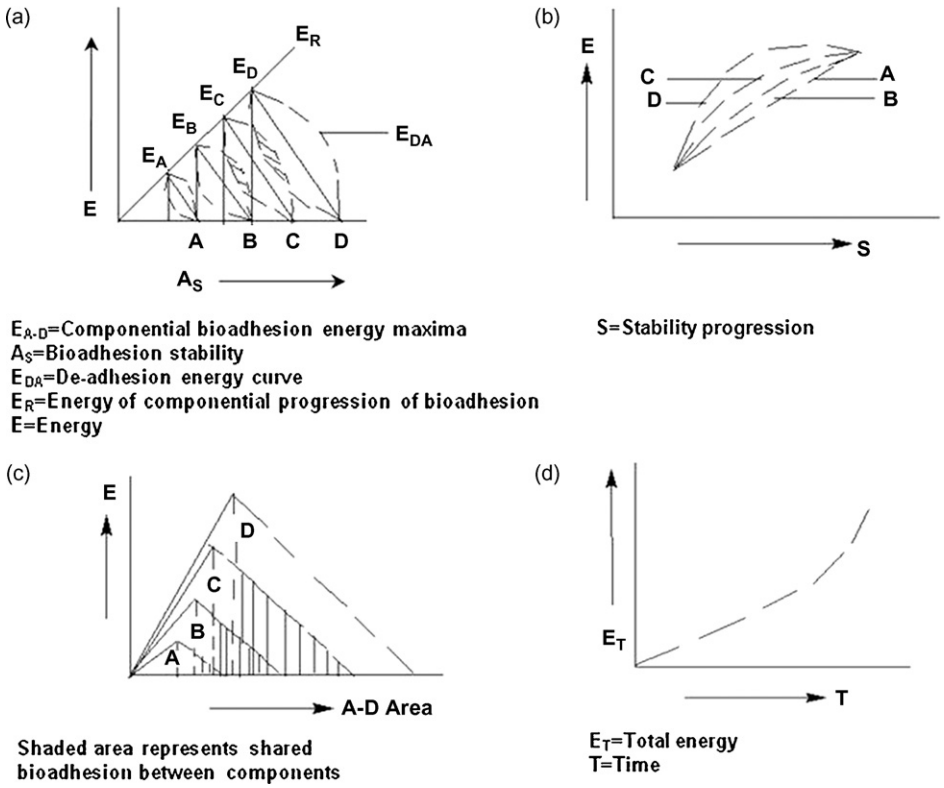

Fig. 8. Energy estimates for the mechanism of bioadhesion. (a) Compartment A = interactions at physical forces levels, B = ionic interactions and ion-exchanges producing bioadhesion, C = chemical interaction involving covalent bonding between the xenobiotic polymer and cellular protein, and D = interaction with surface collagen in the tissue substrate includes polymer–protein–collagen interactions.

sient effect of London forces. Once the caplet and vaginal tissue substrate diffusively merged both interfaces were miscible through a sintering-like mechanism. The strength of bioadhesion depended on a hybrid between the dispersive and diffusive phases as well as the contact surface area. Polymers such as the AS-PAA and APE-PAA were able to significantly wet during sol–gel interconversion and therefore provided a reduced contact angle facilitating bioadhesion.

Fig. 8a–d depicts the energy estimates for bioadhesion representing the physical forces, ionic and chemical interactions as well as ion-exchanges during bioadhesion. This involved electron donations and sharing of covalent bonds between the xenobiotic polymers of the caplet and cellular proteins of the vaginal tissue substrate. Interactions with collagen in the substrate surface with polymer–protein interactions were also present. The extent of hydration also played a significant role in gelation of the caplet resulting in ionic interaction pockets that contributed towards bioadhesion. Structural deformities of the caplet and proteins occurred with proteins transitioning into coiling at primary, secondary, tertiary and quaternary structure levels that participated in bonding to the polymers and facilitated bioadhesion.

The energy barrier between the compartmental interactions determined the extent of bioadhesion as a factor of energy (Fig. 8a–d). The protein and polymer bonding at the cell surface via the embedded glyco-protein and other surface proteins played a role in linking the polymer. The saccharide component of the glycol-proteins bonded to the inherent surface protein and available functional groups and to some extent also bonded to the AS-PAA and APE-PAA polymers within the caplet matrices. The energy differences and level played a rate limiting factor in the proposed bioadhesion phenomenon. Helical structural transitions and distortions within the polymer were predicted by molecular modeling and also affected by stereo-orientation though no effects on the coiling or helical turns of the protein were observed. The embedded glyco-proteins were least affected and provided the anchoring groups for polymer–substrate bioadhesion.

Hydration also played a role and facilitated polymeric gelling and induction of ionic interaction pockets that contributed towards bioadhesion. Furthermore collagen was dissolved from the fibrils by proteases and structurally adjusted to the requirements of bioadhesion as a result of polymer–protein and polymer–collagen interactions. Generally, the barriers to break weak physical bonds do not usually exceed 10–20 times the thermal energy, kT (where k is the Boltzmann constant and T is the absolute temperature). The lifetime of these bonds can vary from microseconds to seconds. Hence, polymers form and break these weak physical bonds numerous times during the course of bioadhesion.

The caplets comprised two types of polymeric chain molecules arising from the AS-PAA and APE-PAA within the matrices. In order to predict the mechanisms of cell-matrix bioadhesion it was assumed that both surfaces (i.e. the caplet and vaginal tissue substrate) were two dimensional parallel planar impenetrable surfaces. In addition to polymeric chain molecules, the residual voids between the two surfaces were assumed to be filled with simulated vaginal fluid. To simulate protein interactions with the polymers, “generic” amino acids were employed and conformations chosen randomly from sterically allowable regions using dihedral angles. The polymer molecules were simulated with a similar strategy. Bioadhesive mechanisms were modeled to capture the essential features of polymer–protein interactions. Increasing the number of sampled conformations did not significantly alter the results and for simplicity only interactions between polymer–protein, collagen–polymer and polymer–protein–collagen were considered with self-interaction terms ignored. All interaction terms con-

tained attractive and repulsive phases with an incompressibility condition or volume-filling constraint introduced to account for repulsive interactions. Under this assumption, no two segments could occupy the same volume which was the result of repulsive interactions.

4. Conclusions

The polymer-based caplets adhered to the simulated vaginal membranes and the freshly excised rabbit vaginal tissue revealing the potential for application in intravaginal drug delivery. Chemometrical and molecular structural modeling deduced that the potential mechanisms of bioadhesivity are a combination of mechanical, chemical, dispersive and diffusive bioadhesive phenomena. Rheological analysis revealed that AS-PAA and APE-PAA displayed varying rheological behavior contributing to bioadhesion to the *in vitro* and *ex vivo* substrates evaluated. Furthermore, the results demonstrated that APE-PAA caplets were more bioadhesive than the AS-PAA caplets and therefore may be more suitable for intravaginal drug delivery applications. The bioadhesivity testing approach employed using freshly excised rabbit vaginal tissue suggests that the method developed may be useful for measuring the bioadhesivity of intravaginal drug delivery systems on vaginal tissue substrates. Rational design of future bioadhesive intravaginal drug delivery systems should focus on the polymer properties that conform to vaginal retention to target bioactives more appropriately.

Ethical approval

Ethics clearance was obtained from the Animal Ethics Committee of the University of the Witwatersrand for this study (Ethics Clearance No. 2007/25/05).

Acknowledgements

This research is supported by Norwegian Agency for Development Co-operation (NORAD)-Norway, National Research Fund (NRF) and a grant from the Faculty Research Committee, University of Witwatersrand, Johannesburg, South Africa.

References

Al-Tahami, K., Singh, J., 2007. Smart polymer based delivery systems for peptides and proteins. Recent Patents Drug Deliv. Formulation 1, 65–71.
Bilensoy, E., Rouf, M.A., Vural, I., Sen, M., Hincal, A.A., 2006. Mucoadhesive, thermosensitive, prolonged-release vaginal gel for clotrimazole: β-cyclodestrin complex. AAPS PharmSciTech. 7, 38.
Bogentoft, C., Carlsson, A., 1996. Gel forming liquid carrier composition, US Patent 5,492,937. http://www.freepatentsonline.com/5492937.html (accessed May 16, 2008).
Bonferoni, M.C., Giunchedi, P., Scalia, S., et al., 2006. Chitosan gels for the vaginal delivery of lactic acid: relevance of formulation parameters to mucoadhesion and release mechanisms. AAPS PharmSciTech. 7, E1–E8.
Ceschel, G.C., Maffei, P., Lombardi, B.S., Ronchi, C., Rossi, S., 2001. Development of a mucoadhesive dosage form for vaginal administration. Drug Dev. Ind. Pharm. 6, 541–547.
Deryaguin, B.V., Toporov, Y.P., Mueler, V.M., Aleinikova, I.N., 1997. On the relationship between the electrostatic and molecular component of the adhesion of elastic particles to a solid surface. J. Colloid Interf. Sci. 58, 528–533.
Desphande, A., Rhodes, C.T., Danish, M., 1992. Intravaginal drug delivery. Drug Dev. Ind. Pharm. 18, 1225–1279.
Elson, C., Milne, A., Curran, D., Kydonieus, A.N., 2000. O-carboxymethylchitosan as a mucoadhesive for vaginal delivery of levonorgestrel. Proc. Int. Symp. Control Rel. Bioact. Mater. 27, 7201–7202.
Furuhjelm, M., Karlgren, C., Carlstrom, K., 1980. Intravaginal administration of conjugated estrogens in postmenopausal women. Int. J. Gynecol. Obstet. 17, 335–339.
Genc, L., Oguzlar, C., Güler, E., 2000. Studies on vaginal bioadhesive tablets of acyclovir. Pharmazie 55, 297–299.
Gilsenan, P.M., Richardson, R.K., Morris, E.R., 2003a. Associative and seggregative interactions between gelation and low methoxy pectin. Part I. Associative interactions in the absence of Ca^{+}. Food Hydrocolloids 17, 723–737.
Gilsenan, P.M., Richardson, R.K., Morris, E.R., 2003b. Associative and seggregative interactions between gelation and low methoxy pectin. Part II. Co-gelation in the presence of Ca^{+}. Food Hydrocolloids 17, 739–749.
Gilsenan, P.M., Richardson, R.K., Morris, E.R., 2003c. Associative and seggregative interactions between gelation and low methoxy pectin. Part III. Quantitative analysis of co-gel moduli. Food Hydrocolloids 17, 751–761.
Helfand, E., Tagami, Y., 1972. Theory of the interface between immiscible polymers. J. Chem. Phys. 57, 1812–1815.
Hussain, N., 2000. Bioadhesive drug delivery systems: fundamentals, novel approaches and development. Int. J. Pharm. 205, 201–202.
Jast, B., Li, X., Clearly, G., 2003. Recent advances in mucoadhesive drug delivery systems. Drug Deliv. Polym. 1, 194–196.
Kaelble, D.H., 1977. A surface energy analysis of bioadhesion. Polymer 18, 475–482.
Kalugin, O.N., Volobuev, M.N., Ischenko, A.V., Adya, A.K., 2001. Structure and dynamics of Na^{+} and Cl^{-} salvation shells in liquid DMSO: molecular dynamics simulations. J. Mol. Liq. 91, 135–148.
Kast, C.E., Valenta, C., Leopold, M., Bernkop-Schnürch, A., 2002. Design and in vitro evaluation of a novel bioadhesive vaginal drug delivery system for clotrimazole. J. Control Rel. 81, 347–354.
Kolawole, O.A., Pillay, V., Choonara, Y.E., 2007. Novel polyamide 6,10 variants synthesized by modified interfacial polymerization for application as a rate-modulated monolithic drug delivery System. J. Bioact. Comp. Polym. 22, 281–313.
Lee, W.J., Park, J.H., Robinson, J.R., 2000. Biodhesive-based dosage forms: the next generation. Am. Pharm. Assoc. J. Pharm. Sci. 89, 850–866.
Lehr, C.M., 2000. Lectin-mediated drug delivery: the second generation of bioadhesive. J. Control Rel. 65, 19–29.
Longer, M.A., Robinson, J.R., 1986. Fundamental aspects of bioadhesion. Pharm. Int. 7, 114–117.
Mandal, T.K., 2000. Swelling-controlled release system for the vaginal delivery of miconazole. Eur. J. Pharm. Biopharm. 50, 337–343.
Mikos, A.G., Peppas, N.A., 1986. Proceed. Int. Symp. Control Rel. Bioact. Mater. 13, 97.
Mikos, A.G., Peppas, N.A., 1990. Scaling concepts and molecular theories of the adhesion of synthetic polymers to glycoproteins. In: Lenaerts, V., Gurny, R. (Eds.), Bioadhesive Drug Delivery Systems. CRC Press, Boca Raton, FL, pp. 25–42.
Nelson, A.L., 2008. The vagina: new options for the administration of medications. http://www.medscape.com/viewarticle/504375.6 (accessed March 10).
Park, K., 1989. A new approach to study mucoadhesion: colloidal gold staining. Int. J. Pharm. 53, 209–217.
Park, K., Robinson, J.R., 1984. Bioadhesive polymers as platforms for oral controlled drug delivery: method to study bioadhesion. Int. J. Pharm. 19, 107–127.
Park, H., Robinson, J.R., 1987. Mechanisms of mucoadhesion of poly(acrylic acid) hydrogels. Pharm. Res. 4, 457–464.
Peppas, N.A., Buri, P.A., 1985. Surface, interfacial and molecular aspects of polymer bioadhesion on soft tissues. J. Control Rel. 2, 257–275.
Picout, D.R., Richardson, R.K., Rolin, C., Abeysekera, R.M., Morris, E.R., 2000a. Ca^{++} induced gelation of low methoxy pectin in the presence of oxidized starch. Part I. Collapse of network structure. Carbohydrate Polym. 43, 113–122.
Picout, D.R., Richardson, R.K., Morris, E.R., 2000b. Co-gelation of calcium pectinate with potato maltodextrin. Part I. Network formation on cooling. Carbohydrate Polym. 43, 133–141.
Repka, M.A., McGinity, J.W., 2001. Bioadhesive properties of hydroxyproplycellulose topical films produced by hot-melt extrusion. J. Control Rel. 70, 341–351.
Robinson, J.R., Bologna, W.J., 2002. Use of polycarboxylic acid polymers to treat vaginal infections, US Patent 6,017,521. http://www.freepatentsonline.com/6017521.html (accessed March 15, 2008).
Santos, C.A., Jacob, J.S., Hertzog, B.A., et al., 1999. Correlation of two bioadhesive assays: the averted sac technique and the CAHN microbalance. J. Control Rel. 61, 113–122.
Schroeder, G., Leska, B., Brzezinski, B., 1998. Solvent effect for proton transfer reaction from dimethyl(4-nitrophenyl)malonate to cis 1,2-bis(dimethylaminomethyl) cyclohexane. J. Mol. Struct. 446, 235–239.
Semalty, A., Semalty, M., 2008. Mucoadhesive polymers—a review. http://www.pharmainfo.net/reviews/mucoadhesive-polymers-review (accessed February 28, 2008).
Smart, J.D., Kellaway, I.W., 1982. *In vitro* techniques for measuring mucoadhesion. J. Pharm. Pharmacol. 34, 70–170.
Smart, J.D., Kellaway, I.W., Worthington, H.E.C., 1984. An *in vitro* investigation of muco-adhesive materials for use in controlled delivery. J. Pharm. Pharmacol. 36, 295–299.
Steinberg, M.S., 1996. Adhesion in development: An historical overview. Dev. Biol. 180, 377–388.
Tang, C., Yin, C., Pen, Y., et al., 2005. New superporous hydrogels composites based on aqueous Carbopol® solution (SPHCcs): synthesis, characterization and *in vitro* bioadhesive force studies. Eur. Polym. J. 41, 557–562.
Ugwoke, M.I., Exaud, S., Van Den Mooter, G., Verbeke, N., Kinget, R., 1999. Bioavailability of apomorphine following intranasal administration of mucoadhesive drug delivery systems in rabbits. Eur. J. Pharm. Sci. 9, 213–219.
Valenta, C., 2005. The use of mucoadhesive polymers in vaginal delivery. Adv. Drug Deliv. Rev. 57, 1692–1712.
Valenta, C., Kast, C.E., Harich, I., Bernkop-Schnürch, A., 2001. Development and *in vitro* evaluation of a mucoadhesive vaginal delivery system for progesterone. J. Control Rel. 77, 323–332.

Valenta, C., Marschütz, M., Egyed, C., Bernkop-Schnürch, A., 2002. Evaluation of the inhibitory effect of thiolated poly(acrylates) on vaginal membrane bound aminopeptidase. J. Pharm. Pharmacol. 54, 603–610.
Vermani, K., Garg, S., 2000. The scope and potential of vaginal drug delivery. Pharm. Sci. Tech. Today (PSTT) 3, 359–364.
Wong, C.F., Yuen, K.H., Peh, K.K., 1999. Formulation and evaluation of controlled release Eudragit® buccal patches. Int. J. Pharm. 178, 11–22.
Yu, Z., Quinn, P.J., 1998. Solvation effects of dimethyl sulfoxide on the structure of phospholipids bi-layers. Biophys. Chem. 70, 35–39.